

Generation of terahertz radiation using zinc oxide as photoconductive material excited by ultraviolet pulses

Shingo Ono,^{a),b)} Hidetoshi Murakami, Alex Quema,^{c)} and Gilbert Diwa^{b)}
Institute for Molecular Science, Myodaiji, Okazaki, Aichi 444-8585, Japan

Nobuhiko Sarukura

Institute of Laser Engineering, Osaka University, Yamadaoka, Suita, Osaka 565-0871, Japan

Ryujiro Nagasaka and Yo Ichikawa

Nagoya Institute of Technology, Showa, Gokiso, Nagoya 466-8555, Japan

Hiraku Ogino, Eriko Ohshima, Akira Yoshikawa, and Tsuguo Fukuda

Institute of Multidisciplinary Research for Advanced Materials, Tohoku University, 2-1-1 Katahira, Aoba-ku, Sendai 980-8577, Japan

(Received 29 April 2005; accepted 3 November 2005; published online 27 December 2005)

Terahertz (THz) radiation generated from photoconductive antenna fabricated on a single crystal zinc oxide (ZnO) is presented. The THz-radiation power is saturated at bias voltages above 800 V/cm and the obtained spectrum extends up to 1 THz. Moreover, ZnO is found to be highly transparent in the visible, near-infrared, mid-infrared and THz frequency regions. The results depicted here will categorically unravel the prospects of using ZnO as a material for integrated active optics. © 2005 American Institute of Physics. [DOI: 10.1063/1.2158514]

The generation of terahertz (THz) pulses from a photoconductive switch was initially demonstrated for the first time using radiation-damaged silicon on sapphire crystals.¹ Subsequently, various materials have been used for photoconductive antennas such as low temperature grown GaAs.^{2,3} Simply increasing the applied bias voltage improves the output power from a photoconductive switch since the electric fields acting on the photoexcited carriers are enhanced. However, this THz enhancement method is constrained by the maximum applied bias voltage, which is limited by the dielectric breakdown of the material. For this reason, wide band gap materials with higher breakdown voltages are potential candidates for photoconductive antennas that operate as high power THz radiation emitters. Recently, high-power THz radiation emitted from a diamond photoconductive antenna array was demonstrated.⁴ The results show that the breakdown electric field of diamond was 2 MV/cm. A diamond photoconductive switch requires a KrF excimer laser as an excitation source since its band gap is located in the deep ultraviolet (UV) region (5.5 eV).⁵ The excitation source is disadvantageous due to the size, running cost, and stability. In addition, a chemical vapor deposited polycrystalline diamond has a smaller mobility (1–70 cm²/V s) than single diamond crystal (1800 cm²/V s).⁴ Unlike diamond, ZnO can be excited by the second or third harmonics of a Ti:sapphire laser. Due to the recent developments of new nonlinear crystals such as CsLiB₆O₁₀, Li₂B₄O₇, BaB₂O₄, and LiB₄O₇,^{6–8} this laser system is significantly efficient. Additionally, efficient UV gain media, which include Ce³⁺:LiCaAlF₆(Ce:LiCAF) and Ce³⁺:LiLuF₄, have been developed.^{9–12} All these works demonstrate that a solid-state UV excitation source is indeed well established.

In this letter, we report on the THz generation from a ZnO photoconductive antenna excited by UV pulses. Due to its highly transparent nature in the visible, near-infrared, mid-infrared, and THz frequency regions, this work demonstrates that ZnO is a suitable hybrid optical material for integrated active optics.

ZnO has attracted considerable interest in the development of blue and UV light emitting devices.^{13,14} Large-sized and high quality crystals are essential for substrates in light emitting devices. Recently, the improved crystal growth techniques have led to the fabrication of substantially large single crystals. In particular, the hydrothermal method has allowed large-sized ZnO single crystals to be grown,¹⁵ which allows flexibility when designing optics in the THz region, including focusing optics and lens duct.¹⁶ As shown in Fig. 1(a), a ZnO crystal has a high transmittance in the THz region. And the periodic structure is attributed to the interference of the signals, which originate from the front and back surfaces of the ZnO crystal. The solid circles indicate the refractive index of ZnO calculated by the fringe gap. A strong dispersion of refractive index is not observed in the 0.3–1.1 THz frequency regions. Assuming refractive index $n=2.9$, the dotted curve is the least-square fitting solution for the transmittance T expressed as¹⁷

$$T = \frac{(1 - R_0)^2 e^{-\alpha d}}{(1 - R_0 e^{-\alpha d})^2 + 4R_0 e^{-\alpha d} \sin^2 \frac{2\pi}{\lambda} nd}, \quad (1)$$

where $R_0 = \frac{(n-1)^2 + \kappa^2}{(n+1)^2 + \kappa^2}$ is the reflectance and $\alpha = \frac{4\pi\kappa}{\lambda}$ is the absorption coefficient. Here, the sample thickness is $d=0.5$ mm, κ is the attenuation coefficient and λ is the wavelength. From this result, κ as fitting parameter is evaluated to be 0.0018. The THz radiation used to obtain the transmission spectrum of ZnO was generated from an InAs semiconductor surface irradiated with femtosecond pulses under a magnetic field with a spectrum central frequency of 0.3 THz.^{18,19} The absorption coefficient at 0.3 THz was evaluated to be

^{a)} Author to whom correspondence should be addressed; electronic mail: shingo@ims.ac.jp

^{b)} Also with the Department of Photo Science, The Graduate University for Advanced Studies, Hayama, Japan.

^{c)} Also with the Department of Physics, De La Salle University, Taft Avenue, Manila 1004, Philippines.

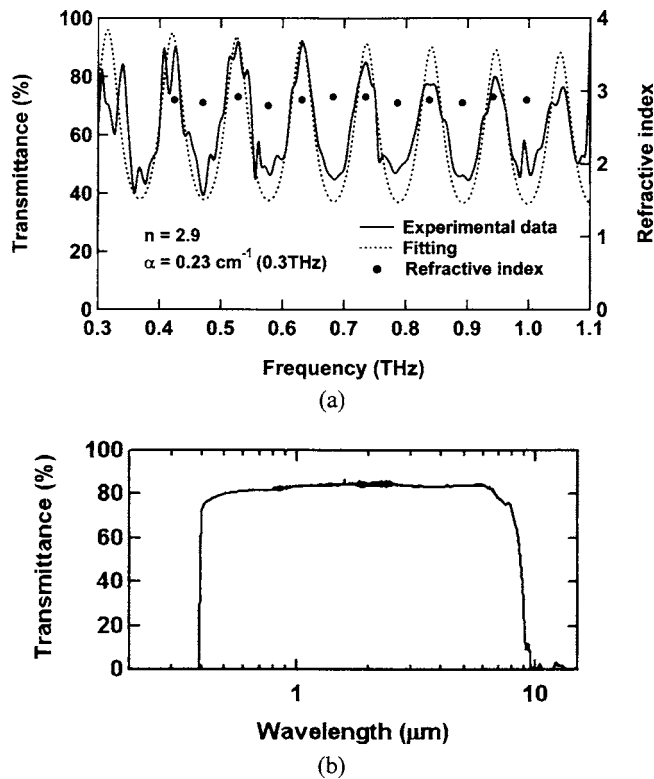


FIG. 1. (a) Transmission spectrum of a ZnO single crystal in the THz region. The periodic structure is due to the interference from the front and back surfaces of the ZnO crystal. (b) Transmission spectrum in the visible, near-infrared and mid-infrared regions.

0.23 cm^{-1} . In addition to its high transmission characteristic in the THz region, ZnO is also transparent in the visible, near-infrared and mid-infrared regions as shown in Fig. 1(b). Unlike silicon and germanium, such high transparency suggests the possibility of using this material for integrated hybrid optics and waveguide. Previously, we demonstrated the THz pigtail that consists of a THz emitter, lens duct, and photonic crystal fiber.^{16,20} For the lens duct, the material should have a high transparency in the near-infrared and THz regions along with a high refractive index. TPX, a polymer based on poly 4-methyl pentene-1, was used as a material of lens duct. The refractive index of TPX is 1.4 in the THz region.¹⁶ It was found that ZnO is better than TPX, which is reasonable since a material with a higher refractive index is more ideal for lens ducts.

The ZnO crystals are of interest as photoconductive material for THz generation due to the ease of fabrication, wide band gap character and relatively high mobility and resistivity. In terms of mobility, ZnO ($200 \text{ cm}^2/\text{V s}$)²¹ is one order of magnitude greater than that of polycrystalline diamond ($1\text{--}70 \text{ cm}^2/\text{V s}$).⁴ ZnO also has the capacity to be excited by the second harmonics of a Ti:sapphire laser since its transmission edge is at 390 nm (3.2 eV band gap). All these qualities make ZnO a suitable candidate for a high power THz emitter.

In our experiment, the frequency tripling of the Ti:sapphire regenerative amplifier output, which has a 290 nm wavelength, was used as the excitation source. High peak power laser pulses can be easily obtained in the 280–330 nm region using a Ce:LiCAF crystal as a gain medium. Femtosecond pulses with a 1 kHz repetition rate had an average output power of 25 mW with a pulse duration of 200 fs. The

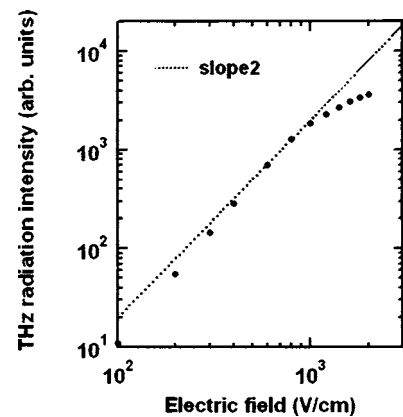


FIG. 2. THz-radiation power dependence on the electric field. Saturation is observed above 800 V/cm.

ZnO single crystals, which were substrates for photoconductive antennas, had dimensions of $10 \times 10 \times 0.5 \text{ mm}$ and the crystallographic c axis of the crystals was oriented parallel to the excitation laser. Two parallel 5-mm-long and 1-mm-wide coplanar silver strip lines were fabricated onto these substrates. The gap between the transmission lines was 1 mm. The excitation laser was focused on the anode side using a 100 mm focal length cylindrical lens. The laser spot size on the sample surface was about $1 \text{ mm} \times 5 \text{ mm}$. A liquid-helium-cooled germanium bolometer was used to detect the total transmitted THz-radiation power.

Figure 2 shows that the THz-radiation power quadratically depends on the electric field. The sample is biased up to 2000 kV/cm and is saturated above 800 V/cm. The saturation is attributed to the increased dark current. It is predicted that the dark current will decrease under high bias voltage and the THz-radiation power will increase as the crystal quality is improved. Figure 3 is the spectrum of the THz radiation obtained by using a polarizing-Michelson interferometer and clearly shows that the spectrum extends up to 1 THz with a peak frequency centered at around 0.35 THz. Clear water vapor absorption lines are observed.²² The main lines are shown as solid lozenge.

In conclusion, we have successfully generated THz pulses from a photoconductive antenna fabricated on ZnO single crystals. Using an all-solid state UV femtosecond laser as the excitation source for ZnO reveals that the THz-radiation power is saturated above 800 V/cm and that the spectrum range extends up to 1 THz. Furthermore, the high transparent nature of ZnO is manifested in the near-infrared and THz frequency regions. These observed characteristics open up the possibility of using ZnO in integrated active optics.

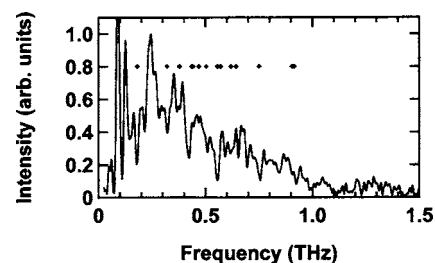


FIG. 3. THz radiation spectrum from a ZnO photoconductive switch.

This research was partially supported by a Grant-in-Aid for Creative Scientific Research, a Grant-in-Aid for Young Scientists (B) (16760043), a Grant-in-Aid for Creative Scientific Research (17GS0209), a Grant-in-Aid for Scientific Research on Priority Areas (16032216), a Grant-in-Aid for Creative Scientific Research Collaboration on Electron Correlation (13NP0201), a Grant-in-Aid for Scientific Research (B) (17360029), Special Coordination Funds for Promoting Science and Aid Technology from the Ministry of Education, Culture, Sports, Science and Technology (MEXT) and a Grant-in-Aid for JSPS Fellows (16-04077) from Japan Society for the Promotion of Science (JSPS).

¹D. Auston and P. Smith, Appl. Phys. Lett. **43**, 631 (1983).

²S. Gupta, J. Whitaker, and G. Mourou, IEEE J. Quantum Electron. **28**, 2464 (1992).

³M. Tani, M. Matsuura, and K. Sakai, Appl. Opt. **36**, 7853 (1997).

⁴H. Yoneda, K. Tokuyama, K. Ueda, H. Yamamoto, and K. Baba, Appl. Opt. **40**, 6733 (2001).

⁵Y. Nabekawa, K. Kondo, N. Sarukura, K. Sajiki, and S. Watanabe, Opt. Lett. **18**, 1922 (1993).

⁶Y. Mori, I. Kuroda, S. Nakajima, T. Sasaki, and S. Nakai, Jpn. J. Appl. Phys., Part 2 **34**, L296 (1995).

⁷R. Komatsu, T. Sugawara, K. Sassa, N. Sarukura, Z. Liu, S. Izumida, Y. Segawa, S. Uda, T. Fukuda, and K. Yamanouchi, Appl. Phys. Lett. **70**, 3492 (1997).

⁸Y. Suzuki, S. Ono, H. Murakami, T. Kozeki, H. Ohtake, N. Sarukura, G. Masada, H. Shiraiishi, and I. Sekine, Jpn. J. Appl. Phys., Part 2 **41**, L823 (2002).

⁹M. Dubinskii, V. Semashko, A. Naumov, R. Abdulsabirov, and S.

Korableva, J. Mod. Opt. **40**, 1 (1993).

¹⁰Z. Liu, T. Kozeki, Y. Suzuki, N. Sarukura, K. Shimamura, T. Fukuda, M. Hirano, and H. Hosono, Opt. Lett. **26**, 301 (2001).

¹¹S. Ono, Y. Suzuki, T. Kozeki, H. Murakami, H. Ohtake, N. Sarukura, H. Sato, S. Machida, K. Shimamura, and T. Fukuda, Appl. Opt. **41**, 7556 (2002).

¹²N. Sarukura, Z. Liu, Y. Segawa, K. Edamatsu, Y. Suzuki, T. Itoh, V. V. Semashko, A. K. Naumov, S. L. Korableva, R. Y. Abdulsabirov, and M. A. Dubinskii, Opt. Lett. **20**, 294 (1995).

¹³A. Tsukazaki, A. Ohtomo, T. Onuma, M. Ohtani, T. Makino, M. Sumiya, K. Ohtani, S. F. Chichibu, S. Fuke, Y. Segawa, H. Ohno, H. Koinuma, and M. Kawasaki, Nat. Mater. **4**, 42 (2005).

¹⁴H. Ohta, K. Kawamura, M. Orita, M. Hirano, N. Sarukura, and H. Hosono, Electron. Lett. **36**, 984 (2000).

¹⁵E. Ohshima, H. Ogino, I. Niikura, K. Maeda, M. Sato, M. Ito, and T. Fukuda, J. Cryst. Growth **260**, 166 (2004).

¹⁶G. Diwa, A. Quema, E. Estacio, H. Murakami, S. Ono, R. Pobre, and N. Sarukura, Appl. Phys. Lett. (submitted).

¹⁷M. Born and E. Wolf, in *Principles of Optics* (Cambridge University Press, Cambridge, 1998) pp. 323–329.

¹⁸X. C. Zhang, Y. Lin, T. Hewitt, T. Sangsiri, L. Kingsley, and M. Weiner, Appl. Phys. Lett. **62**, 2003 (1993).

¹⁹N. Sarukura, H. Ohtake, S. Izumida, and Z. Liu, J. Appl. Phys. **84**, 654 (1998).

²⁰M. Goto, A. Quema, H. Takahashi, S. Ono, and N. Sarukura, Jpn. J. Appl. Phys., Part 2 **43**, L317 (2004).

²¹K. Maeda, M. Sato, I. Niikura, and T. Fukuda, Semicond. Sci. Technol. **20**, S49 (2005).

²²H. M. Pickett, R. L. Poynter, and E. A. Cohen, Submillimeter, Millimeter, and Microwave Spectral Line Catalog, accessed via World Wide Web (<http://spec.jpl.nasa.gov>) from the Jet Propulsion Laboratory, Pasadena, California.